

Lawrence Berkeley National Laboratory

Recent Work

Title

THE ATOMIC STRUCTURE OF (001) GRAIN BOUNDARIES AND (001) SURFACES IN $\text{YBa}_2\text{Cu}_3\text{O}_{7-\Delta}$

Permalink

<https://escholarship.org/uc/item/3sw1v36p>

Authors

Zandbergen, H.W.

Gronsky, R.

Thomas, G.

Publication Date

1988-09-01

c.2



Lawrence Berkeley Laboratory

UNIVERSITY OF CALIFORNIA

Materials & Chemical Sciences Division

National Center for Electron Microscopy

Submitted to Journal de Microscopie et du Spectroscopie Electronique

LAWRENCE
BERKELEY LABORATORY

DEC 6 1988

The Atomic Structure of (001) Grain Boundaries and (001) Surfaces in $YBa_2Cu_3O_{7-\delta}$

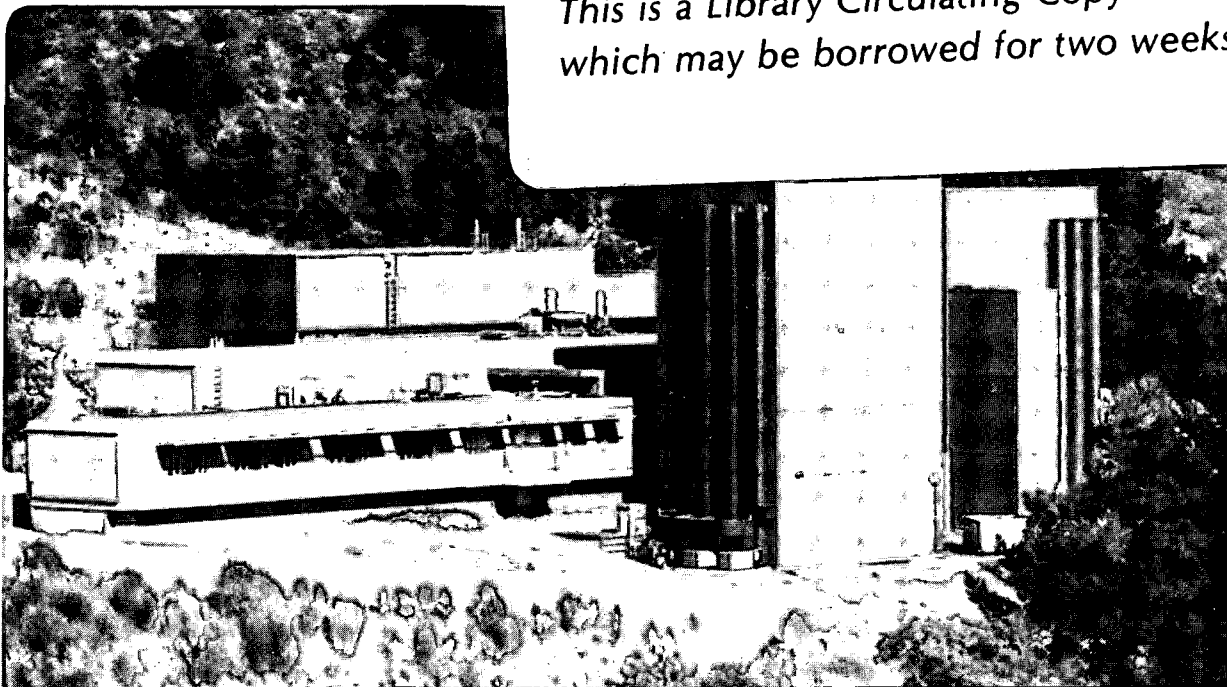
LIBRARY AND DOCUMENTS SECTION

H.W. Zandbergen, R. Gronsky, and G. Thomas

September 1988

TWO-WEEK LOAN COPY

This is a Library Circulating Copy which may be borrowed for two weeks.



LBL-25800
c.2

DISCLAIMER

This document was prepared as an account of work sponsored by the United States Government. While this document is believed to contain correct information, neither the United States Government nor any agency thereof, nor the Regents of the University of California, nor any of their employees, makes any warranty, express or implied, or assumes any legal responsibility for the accuracy, completeness, or usefulness of any information, apparatus, product, or process disclosed, or represents that its use would not infringe privately owned rights. Reference herein to any specific commercial product, process, or service by its trade name, trademark, manufacturer, or otherwise, does not necessarily constitute or imply its endorsement, recommendation, or favoring by the United States Government or any agency thereof, or the Regents of the University of California. The views and opinions of authors expressed herein do not necessarily state or reflect those of the United States Government or any agency thereof or the Regents of the University of California.

THE ATOMIC STRUCTURE OF (001) GRAIN BOUNDARIES AND (001) SURFACES IN $\text{YBa}_2\text{Cu}_3\text{O}_{7-\delta}$.

H.W. Zandbergen^{1,2}, R. Gronsky², and G. Thomas²

1. Gorlaeus Laboratories, State University Leiden, P.O. Box 9502, 2300 RA Leiden, The Netherlands.
2. National Center for Electron Microscopy, Materials and Chemical Sciences Division, Lawrence Berkeley Laboratory, 1 Cyclotron Rd., Berkeley CA 94720, USA

ABSTRACT

High resolution electron microscopy (HREM) studies of grain boundaries and fractured surfaces in both the tetragonal and orthorhombic phases of dense (>90%) $\text{YBa}_2\text{Cu}_3\text{O}_{7-\delta}$ have been performed. Grain boundaries are very often found to be parallel to a (001) plane of one of the adjacent grains, and the structure of the interface is very similar to the structure of the (001) surface of fractured $\text{YBa}_2\text{Cu}_3\text{O}_{7-\delta}$. Matching of experimental and calculated images shows that the surface layer is a deformed BaO layer. Results indicate that the low critical currents observed in sintered materials are caused by textured grain growth in combination with the atomic structure of the grain boundary plane, and the intercalation of off-stoichiometric species near the grain boundary. This work is supported by the Director, Office of Energy Research, Office of Basic Energy Sciences, Materials Sciences Division of the U.S. Dept. of Energy under contract No. DE-AC03-76SF00098.

INTRODUCTION

Phase contrast techniques of high resolution electron microscopy provide a direct image of the atomic structure of most materials under carefully-controlled experimental conditions. This technique has been successfully applied to the analysis of perfect crystals of $\text{YBa}_2\text{Cu}_3\text{O}_{7-\delta}$, yielding excellent agreement with x-ray and neutron scattering data.

However, the strength of the technique is its spatial localization, in particular as applied to the analysis of defects in materials. To date, applications of high resolution electron microscopy to the analysis of defects in $\text{YBa}_2\text{Cu}_3\text{O}_{7-8}$ have been limited to stacking disorders involving the c-planes [1-12]. However, these are very often created at room temperature or during post-sintering heat treatment [2], e.g. annealing at 450°C , and are exaggerated by some preparation techniques [13]. Because most of these planar defects are formed by an intercalation of Cu and O atoms from the surface [2], the resultant strains cause lattice deformations. This lattice bending leads to distortions of the image making their interpretation very difficult and subject to error.

Unfortunately in some early reports [1,3,4,8] this instability of $\text{YBa}_2\text{Cu}_3\text{O}_{7-8}$ was not taken into account, and the observed defects were incorrectly attributed to the as-synthesized material, citing either cation disorder [1,4] or structural deviations important for superconductivity [3,8]. However, later studies showed that in properly-prepared bulk $\text{YBa}_2\text{Cu}_3\text{O}_{7-8}$ the number of planar defects is very low. Evidently in any study of grain boundaries it is very important that the specimens be carefully prepared and screened against the introduction of artificial planar defects.

The study of grain boundaries in these materials is becoming increasingly more important [14-16]. It is well known that grain boundaries are sources of problems in many ceramic materials: they affect mechanical properties such as creep, electronic properties such as ionic conduction in β Na alumina [17,18] and magnetic response such as magnetostriction which can impair soft magnetic properties [19]. Similarly, it should be expected that grain boundaries might affect superconductivity, and any discontinuity in electronic conduction across the boundary plane might account for the relatively poor critical currents observed in sintered specimens. Evidence shows that sintered polycrystalline $\text{YBa}_2\text{Cu}_3\text{O}_{7-8}$ with random grain-to-grain orientation exhibits much lower critical currents than single crystals, typically 10^3 versus 10^6 Amp/cm². This is surprising because the material can be densified up to 94%, and the anisotropy of the critical current (20) can

only account for a relative small drop in J_c due to random grain misorientation. A possible explanation, the existence of an amorphous phase at the grain boundaries, was reported by Nakahara et al [16]. However in all of our investigations no amorphous layer was observed and is therefore ruled out as the only cause of the low critical currents. Detailed high resolution electron microscopy of the grain boundaries was initiated in order to investigate whether the atomic structure at the interface can be the reason for the low critical currents observed in polycrystalline material.

EXPERIMENTAL PROCEDURES

Sample Preparation

Samples were prepared by preheating $\text{YBa}_2\text{Cu}_3\text{O}_{7-8}$ at 850°C for approximately 6 hours then sintering for 2 to 48 hours at 950°C into pellet form. Subsequent annealing at 450°C was carried out for several days to ensure complete uptake of oxygen. Specimens for electron microscopy were prepared by dry grinding to $10\mu\text{m}$ thickness using 320 mesh paper, followed by ion beam thinning using an Ar beam at 4kV and an incident angle of $12-15^\circ$ in a liquid nitrogen cooled stage. To prevent reaction of the samples (13) they were left in the vacuum of the ion milling equipment until they could be transferred into the electron microscope.

Electron Microscopy

High resolution electron microscopy was carried out in a JEOL JEM 200CX electron microscope, equipped with a top entry $\pm 10^\circ$ double-tilt goniometer operating at 200 kV, and the Berkeley Atomic Resolution Microscope [21] equipped with a $\pm 40^\circ$ biaxial, double-tilt goniometer operating at 1000 kV.

EXPERIMENTAL RESULTS

The planar stacking fault observed most frequently in $\text{YBa}_2\text{Cu}_3\text{O}_{7-8}$ is a defect which leads to an increase in the c-axis of about 15%.

Comparisons between simulated images [11,22] and experimental ones indicate that the defect is a $(\text{CuO})_2$ double layer. Ex-situ heating experiments have shown [2] that these defects initiate at internal and exposed surfaces, and are formed by insertion of an extra CuO layer at the site of the original CuO layer between the two BaO layers [11] in the "perfect" structure. An example of the defect is given in Figure 1. A similar structure of double layers is observed in SrCuO_2 [23]. The $(\text{CuO})_2$ double layer is associated with a shift of $a/2$ or $b/2$, both having an approximately equal chance of occurrence. At room temperature, intercalation of the extra Cu and O atoms is restricted to the near-surface layers of the crystal, presumably because of the low diffusion rate of copper and/or oxygen, and because of physical constraints in the bulk since the diffusion is accompanied by expansion and spallation of the lattice. Without such restrictions, it might be expected that complete intercalation can be obtained, leading to a superstructure with twice the number of CuO layers. Such a superstructure has indeed been observed in thin films [23,24] and near grain boundaries in dense sintered material. Examples are given in Figures 2 and 3.

A large number of grain boundaries show the interface of one of the grains to be a low energy (001) plane and had the appearance of being formed by impingement of grain upon grain. Figure 4 shows an example of such a grain boundary in the tetragonal phase $\text{YBa}_2\text{Cu}_3\text{O}_{7-8}$ material. In none of the specimens investigated was any amorphous phase found to be present at the grain boundaries.

Figure 5 shows another grain boundary in tetragonal $\text{YBa}_2\text{Cu}_3\text{O}_{7-8}$. Close inspection of the image reveals that there is an incomplete unit cell, defined here as an intact block of the six-layer sequence $\text{CuO}_2\text{-BaO-CuO-BaO-CuO}_2$, bordering the grain boundary. The image furthermore reveals, after careful processing, that the interface terminates at a BaO layer. A similar termination of the lattice is observed for surfaces obtained by fracturing $\text{YBa}_2\text{Cu}_3\text{O}_{7-8}$, as can be seen in figure 6. This is consistent with the results of XPS measurements of Halbritter *et al* [25], which show the (001) surface to be a BaO₂ plane.

In material sintered at 950°C for 48 hours and annealed at 450°C for 48 hours, both in an oxygen flow, it was observed that near some of the grain boundaries many $(\text{CuO})_2$ double layers were present. This

indicates that using an oxygen flow instead of air for the annealing step encourages the intercalation phenomenon. Regions of both very high and very low defect density were found near grain boundaries, indicating that the boundaries play an essential role in the transport of material necessary for the intercalation process. This is expected because of enhanced diffusion along grain boundaries relative to that within the matrix.

DISCUSSION

The above results show that the atomic stacking sequence in perfect $\text{YBa}_2\text{Cu}_3\text{O}_{7-\delta}$ may be terminated abruptly at those grain boundaries with (001) orientation in such a way that an incomplete unit cell is left at the interface. The structural block observed here, i.e. $\text{CuO}_2\text{-BaO-CuO-BaO}_x$, will have different superconducting properties than the perfect 1-2-3 phase, and in fact may be completely insulating. Since the correlation length of Cooper pairs along the c axis is approximately 0.6 nm (26), such an insulating layer of 1nm thickness can have a strong negative effect on superconduction, especially because it is so abundant. More than 90% of the grain boundaries observed in these materials were parallel to (001) planes of one of the adjacent grains.

Nagahara *et al* [16] investigated materials of 1-2-3 phase with small and large grain sizes. They observed that the large grain material had a plate-like character with an abundance of (001) interfaces and interfacial facets, whereas the small grain material had no distinctive faceting. They also found that the small grain material sustained a considerably higher critical current. This in conflict with their assumption that an amorphous phase is present at the grain boundaries. However it agrees very well with our model, since in the small grain material the number of problematic (001) interfaces at the grain boundaries will be much less. Also the observation of Jin *et al* [27] that c-axis aligned polycrystalline material has a much higher critical current is in agreement with our model. In this case the grain

boundaries will join either two non-conducting (001) interfaces perpendicular to their common c axis, or two conducting (001) interfaces in a direction closely parallel to their common c axis.

Intercalation of an extra CuO layer is found to take place even at room temperature and is enhanced progressively at increasing temperatures. This intercalation was found to take place only along the CuO planes, viz. normal to the c axis and is thus restricted by diffusion of Cu and O from the surface. Investigation of dense orthorhombic material, sintered and annealed for several days, showed that the intercalation can also take place along those CuO planes intersecting the grain boundaries (see figure 3). When the grain interface is a (001) plane, intercalation from that grain boundary obviously cannot occur. Although the volume fraction of the intercalated material might be small, the effect on the critical current will be large, since it is concentrated near the grain boundaries.

Due to the expansion of the c axis caused by the extra CuO layer (~15%), partial intercalation will lead to local lattice bending [2,11]. This lattice distortion causes difficulties in image interpretation, but it also might have a significant effect on superconducting properties. Kapitulnik *et al* [28] report that structurally-modified 1-2-3 phase in which every CuO layer is replaced by a $(\text{CuO})_2$ double layer, in a sense the extreme of the intercalation behavior observed here, leads to the compound $\text{YBa}_2\text{Cu}_3\text{O}_{8.8}$ which has a T_c of approximately 80 K. Unfortunately, partial intercalation and its concomitant lattice distortion might cause strong decreases in the critical temperature and current. One possible cause for poorer superconducting properties in the locally intercalated regions is the detailed structure of the core of the distortion observed at high spatial resolution. At the termination of the intercalated layer there is a bifurcation of the original CuO layer into the two layers comprising the $(\text{CuO})_2$ double layer.

CONCLUSION

The low critical current in polycrystalline material is due to the structure and frequent occurrence of the low energy (001) interface at grain boundaries, and intercalation along the CuO planes that intersect

grain boundaries. Since both phenomena are inherent to the bond strengths in the structure of $\text{YBa}_2\text{Cu}_3\text{O}_{7-\delta}$ the critical current cannot be improved significantly by grain boundary engineering alone.

ACKNOWLEDGEMENTS

This work is supported by the Director, Office of Energy Research, Office of Basic Energy Sciences, Materials Sciences Division of the U.S. Department of Energy under contract No. DE-AC03-76SF00098.

REFERENCES

1. H.W. Zandbergen, G. van Tendeloo, T. Okabe, and S. Amelinckx, *Phys. Stat. Sol.(a)*, **103**, 45 (1987).
2. H.W. Zandbergen, R. Gronsky and G. Thomas, *Phys. Stat. Sol.(a)* **105**, 207 (1988).
3. A. Ourmazd, J.A. Rentschler, J.C.H. Spence, M. O'Keefe, R.J. Graham, D.W. Johnson, Jr., and W.W. Rhodes, *Nature*, **327**, 308 (1987).
4. L. D. Marks, J.P. Zhang, S.-J. Hwu, and K.R. Poeppelmeier, *Journal of Solid State Chemistry*, **69**, 18 (1987).
5. B. Domenges, M. Hervieu, C. Michel, and B. Raveau, *Europhys. Lett.* **4** (2), pp 211-214 (1987).
6. M.P.A. Viegers, D.M. de Leeuw, C.A.H.A. Mutsaers, H.C.A. Smoorenburg, J.H.T. Hengst, J.W.C. de Vries and P.C. Zalm, to be published.
7. Y. Matsui, E. Takayama-Muromachi, A. Ono, S. Horiuchi, and K. Kato, *Jap. J. Appl. Phys.*, **26**, L777, (1987).
8. J. Narayan, V.N. Shukla, S.J. Lukasiewicz, N. Biunno, R. Singh, A.F. Schreiner, and S.J. Pennycook, *Appl. Phys. Lett.*, **51**, 940 (1987).
9. J. Tafto, M. Suenaga, T. Wang, R.L. Sabatini, A.R., Moodenbaugh, and S. Levine, Proc. MRS Fall Meeting Boston (1987).
10. J. Tafto, M. Suenaga, and R.L. Sabatini, Proc. MRS Fall Meeting Boston (1987).

11. H.W. Zandbergen, R. Gronsky, K. Wang, and G. Thomas, *Nature*, **331**, 596 (1988).
12. M. Hervieu, B. Domenges, C. Michel, Herger, J. Provost, and B. Raveau, *Phys. Rev. B*, **36**, 3920, (1987).
13. H.W. Zandbergen, C.J.D. Hetherington, and R. Gronsky, accepted by *Journal of Superconductivity*.
14. H.W. Zandbergen and G Thomas, submitted to *Acta Cryst.*
15. H.W. Zandbergen, R. Gronsky and G. Thomas, Proc. HTSC M2S, Interlaken March 1988.
16. S. Nakahara, G.J. Fisanick, M.F. Yan, R.B. van Dover, and T. Boone, submitted to *Appl. Phys. Lett.*, (1987).
17. S. Sarian, and B.J. Dunbar, and W.J. McEntree, in *Ceramic Microstructures '76*, ed. R.M. Fulrath and J.A. Pask, Westview Press (1976).
18. L.C. DeJonghe, *J. Mat. Sciences* **14**, 33 (1979).
19. I-Nan Lin, R.K. Mishra, and G. Thomas, in *Advances in Materials Characterization*, Plenum Press New York, pp 351, 1983.
20. P. Kes, Proc. Int. Conf. HTSC-M2S Interlaken, 1988.
21. R. Gronsky and G. Thomas, Proc. 41th Ann. Meeting, Elec. Micr. Soc. Amer., G.W. Bailey, ed., Claitor's, Baton Rouge (1983) p 310.
22. L. Marks, Proc. Mat. Res. Soc. Meeting Fall1987 Boston.
23. C.L. Teske, and H. Mueller-Buschbaum, *Z. Anorg. Algem. Chem.*, **379**, 234 (1970).
24. A. F. Marshall, R.W. Barton, K. Shar, A. Kapitulnik, B. Oh, R.H. Hammond, and S.S. Laderman, preprint.
25. J. Halbritter, , Proc. Int. Conf. HTSC-M2S Interlaken, 1988.
26. A. Umezawa et al, submitted to *Phys. Rev. Letters*.
27. S. Jin , Proc. MRS Fall Meeting Boston (1987).
28. A. Kapitulnik, Proc. Int. Conf. HTSC-M2S Interlaken, 1988.

FIGURE CAPTIONS

Figure 1. Example of planar defects in $\text{YBa}_2\text{Cu}_3\text{O}_{7-8}$ viewed along $[010]$. The defects are formed by intercalation of Cu and O, creating a $(\text{CuO})_2$ double layer. Depending upon the shift ($a/2$ or $b/2$) across the layers, two different images are obtained for the same defect as shown here. The figure shows (a) the digitized image, averaged over 10 unit cells along the a axis, (b) the calculated image, (c) the image without any image processing and (d) the model used for the image calculations. More details on the image calculations are given in ref [11] XBB 881-479.

Figure 2. Micrograph of an ion milled thin film (700 nm) on SrTiO_3 substrate, perpendicular to the film plane. Note at the left the large region wherein every CuO layer has been converted to a $(\text{CuO})_2$ double layer XBB 881-482.

Figure 3. Micrograph of a grain boundary in dense $\text{YBa}_2\text{Cu}_3\text{O}_{7-8}$, which has been sintered at 950°C and annealed at 450°C , both treatments conducted for 48 hours in oxygen. The upper grain is approximately 10° off of an exact $[110]$ orientation and the lower grain exactly in the $[100]$ zone. The lower grain has only $(\text{CuO})_2$ double layers in the region shown. Note the continuous bending of the (001) layers over the whole region. Furthermore the grain boundary shows a stepped interface with the $[100]$ grain, whereas the other grain has grown into the steps to complete impingement. The grain boundary remains straight in spite of the severe lattice bending and 15% expansion caused by the intercalation XBB 888-7815.

Figure 4. Micrograph showing a grain boundary in tetragonal $\text{YBa}_2\text{Cu}_3\text{O}_{7-8}$. No amorphous phase is present at the interface XBB 870-10597.

Figure 5. Micrographs showing (a) the structure of the (001) interface at the grain boundary, and (b) the same image after processing. At the

interface a $\text{CuO}_2\text{-BaO-CuO-BaO}_x$ block is present, probably leading to an insulating layer XBB 8711-4633.

Figure 6. The surface of a fractured crystal from polycrystalline $\text{YBa}_2\text{Cu}_3\text{O}_{7-\delta}$. The atomic structure at the surface is similar to that of the grain interface shown in figure 5 XBB 870-10603.

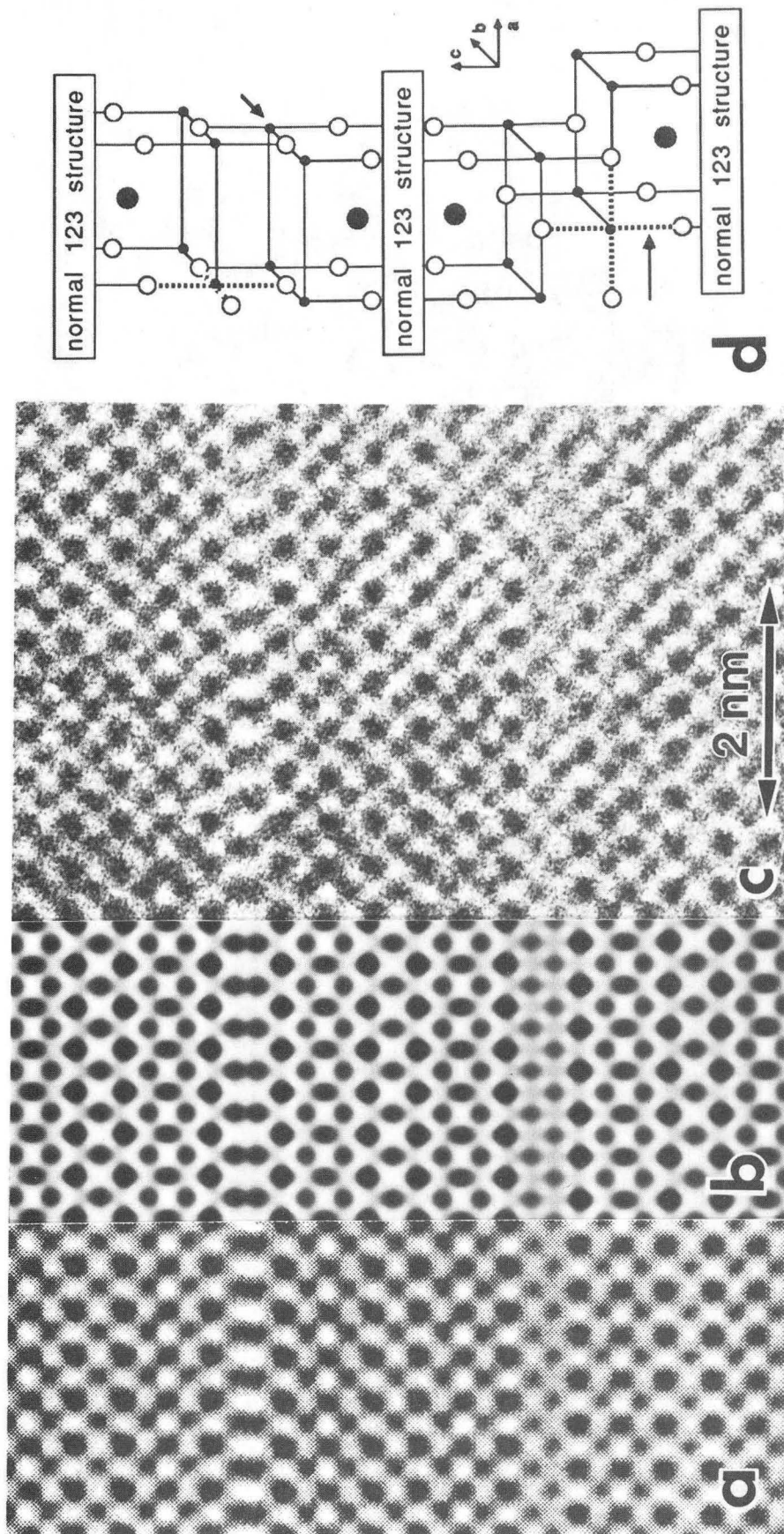


Figure 1

XBB 881-479

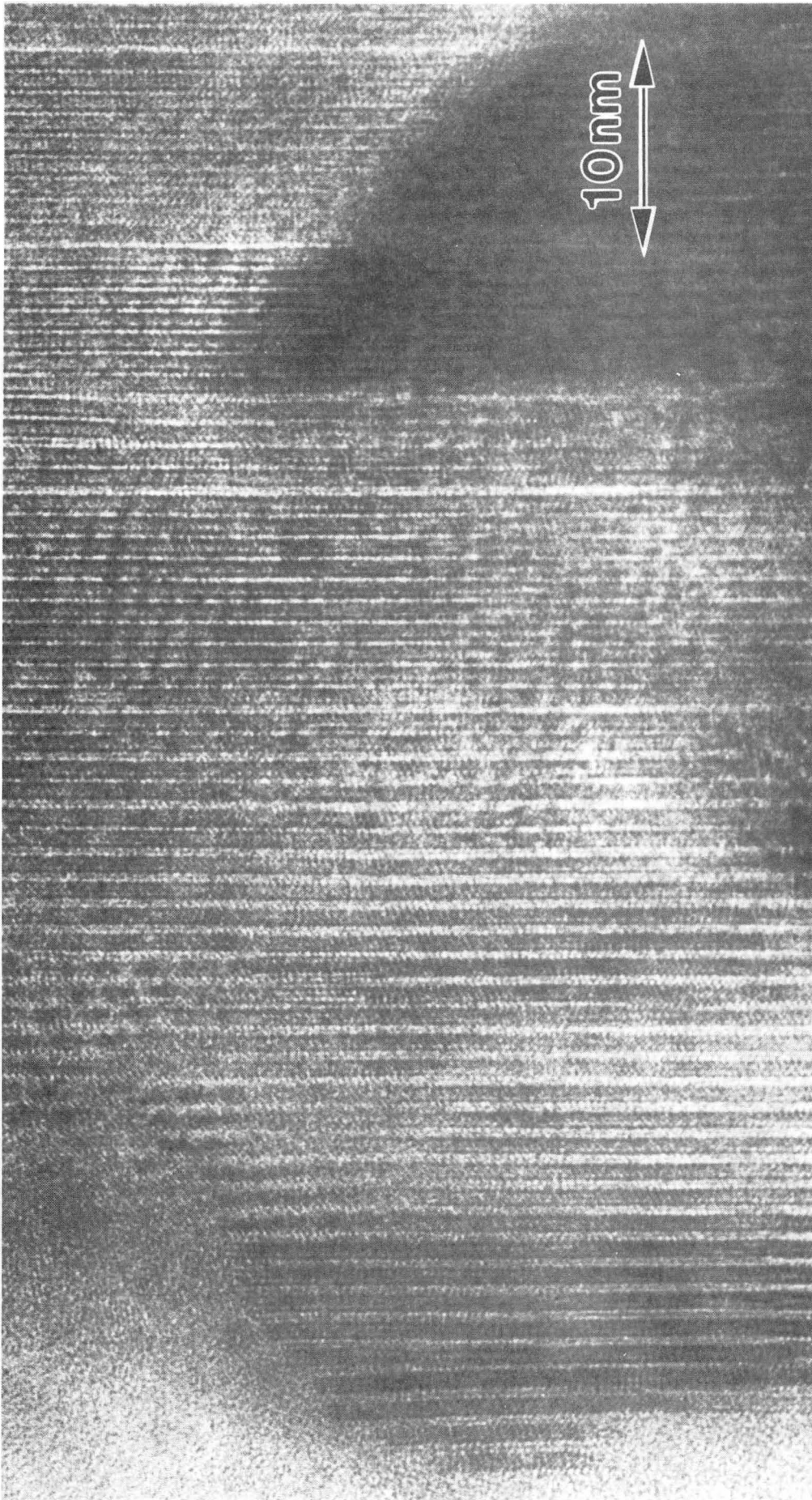


Figure 2

XBB 881-482

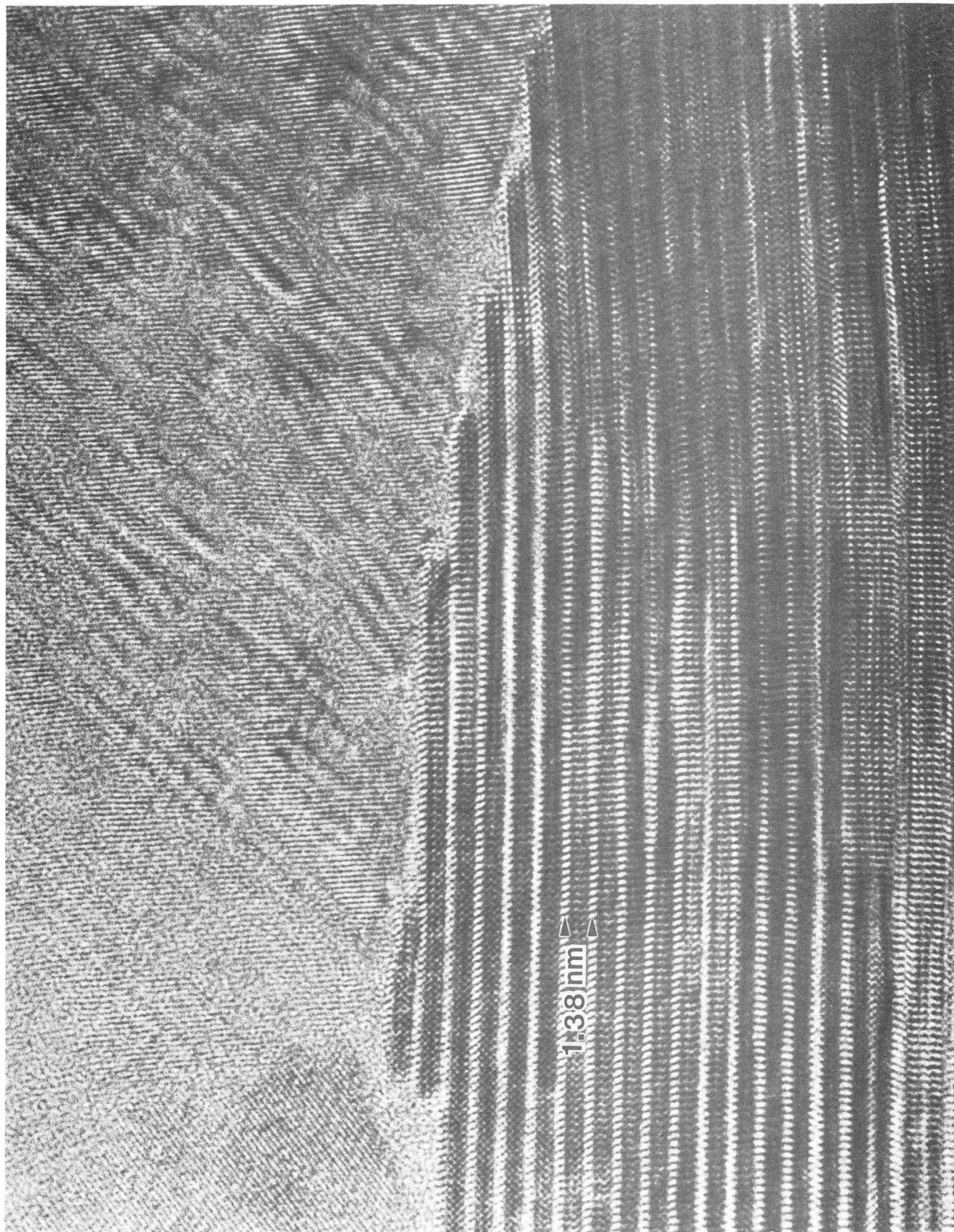


Figure 3

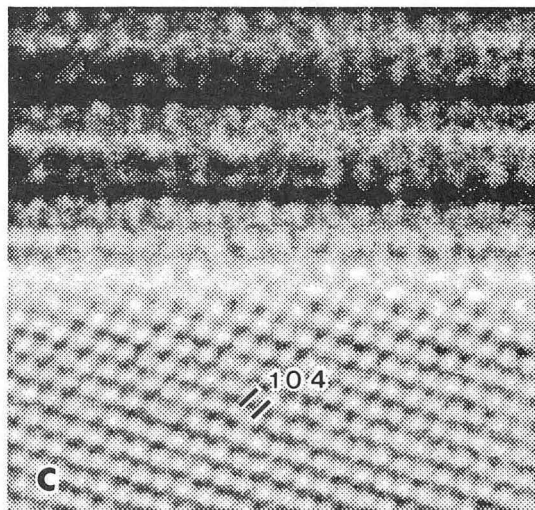
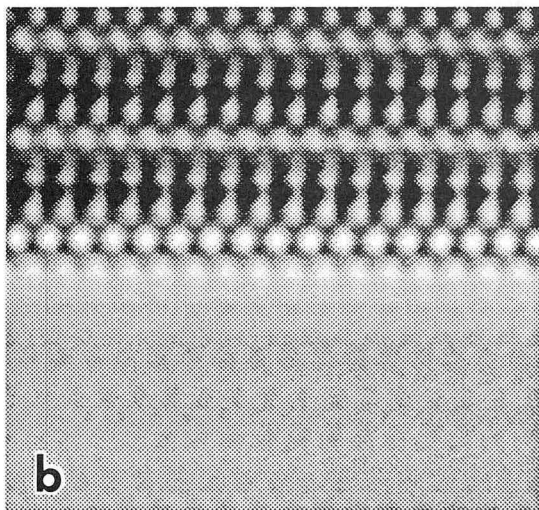
XBB 888-7815

XBB 870-10597

10 nm



Figure 4



XBL 8711-4633

Figure 5

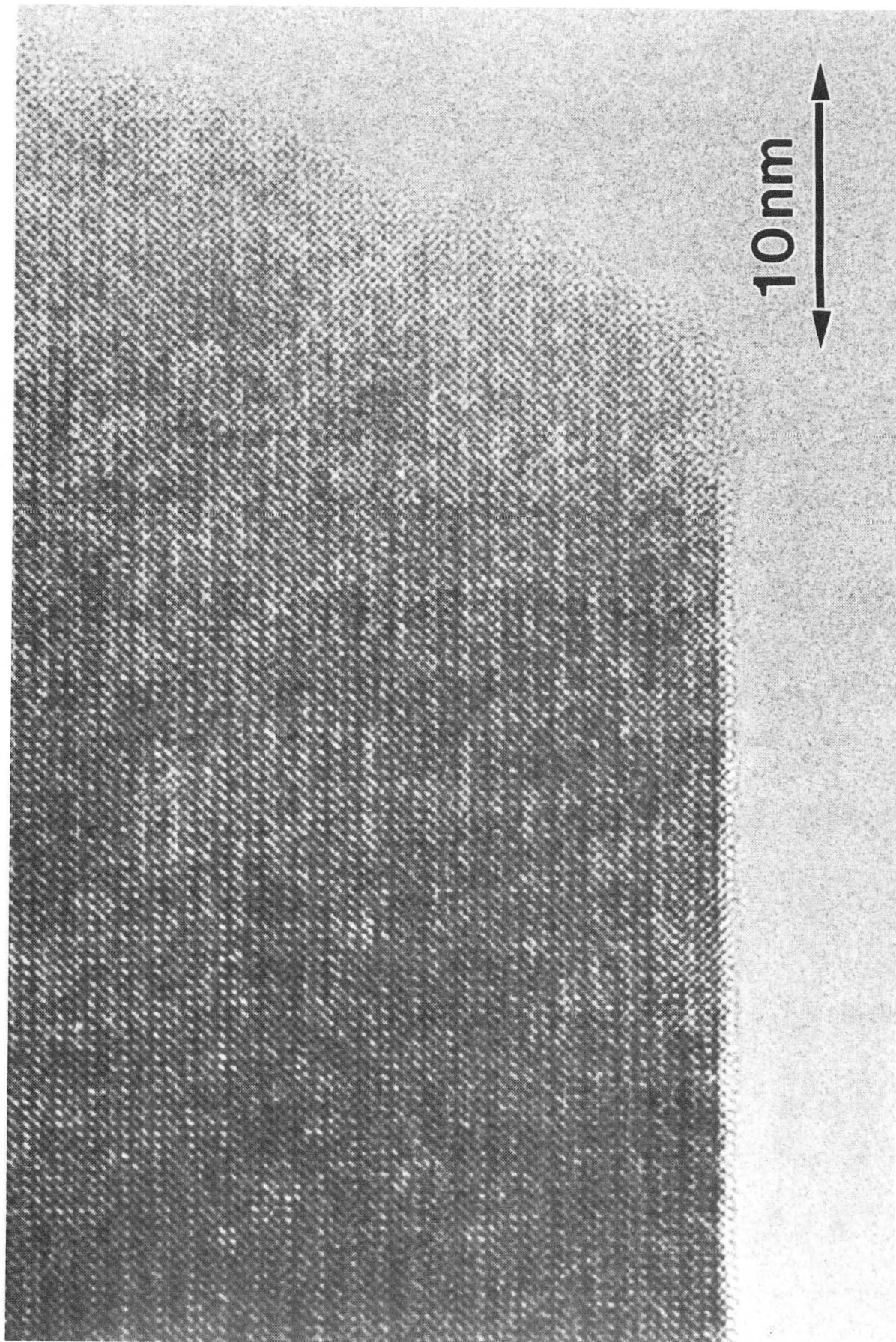


Figure 6

XBB 870-10603

*LAWRENCE BERKELEY LABORATORY
TECHNICAL INFORMATION DEPARTMENT
UNIVERSITY OF CALIFORNIA
BERKELEY, CALIFORNIA 94720*